Int. J. Electrochem. Sci., 11 **(2016)** 843 - 854

International Journal of
ELECTROCHEMICAL
SCIENCE
www.electrochemsci.org

Influence of Three Different Anions on Morphology and Property of Trivalent Chromium Based Conversion Coating on Aluminum Alloy

Xiaolei Ren, Shengtao Zhang[*]*, Siyi Chen, Shenying Xu, Linliang Yin*

School of Chemistry and Chemical Engineering, Chongqing University, Chongqing 400044, P.R. China
[*]E-mail: 1355509739@qq.com

Received: 31 October 2015 / *Accepted:* 17 November 2015 / *Published:* 1 December 2015

The influence of F^-, $C_2O_4^{2-}$ and $Mo_7O_{24}^{6-}$ as film agents on the morphology and the electrochemical property of trivalent chromium based conversion coating was investigated with the methods of scanning electronic microscope (SEM), contact angle measurement and electrochemical test. From the SEM micrograph and contact angle measurement, we observed various morphologies and properties for the Cr(III)-based CCC on aluminum alloy among the specimens immersed in different solutions, and the specimen in Cr(III)/$Mo_7O_{24}^{6-}$ solution displays a much smooth and dense morphology without notable crevices, the value of contact angle is 112.9°. The electrochemical tests showed that the anti-corrosion properties are also varied among the coatings formed in different conversion solution, which is attributed to the different role of each agent. And we also explain the possible formation mechanism under the influence of three different anions. All results demonstrate $Mo_7O_{24}^{6-}$ is the best coating formation agent among the three anions.

Keywords: Anion effect, Morphology, Electrochemical properties, Aluminum alloy

1. INTRODUCTION

Aluminum alloys exhibit excellent mechanical and physical properties as structural materials and thus are widely applied for automotive industry, aircrafts, medical appliances, and electronic equipment. Nevertheless, they are usually prone to local corrosion due to their complex microstructure and the presence of intermediate metal phase[1-5]. Thus, we must perform surface treatments for aluminum alloys to protect the alloy substrate before application. One traditional protection strategy is chromate conversion coating process (CCC), Cr(VI)-based CCC[6-8]. Unfortunately, the Cr(VI)-based CCC involves hexavalent chromium ion, Cr(VI), which is toxic and carcinogenic, and limited by

several environmental legislations. Another alternative strategy for aluminum alloy is the trivalent chromium based conversion coating method, Cr(III)-based CCC[9-11]. The Cr(III)-based CCC process is nontoxic, but its protection efficiency is much lower than that of Cr(VI)-based process[10, 11].Therefore, how to improve the performance of Cr(III)-based CCC is becoming a hot research topic, e.g. the effects of Co(Ⅱ), Ni(Ⅱ), Fe(Ⅱ) to enhance the anti-corrosion performance of Cr(III)-based coating, the diverse structures of Cr(III)-based coating with different chromate salts including chromium nitrate, chromium trichloride and chromium sulfate, etc.[10, 12].

The classical medium for Cr(III)-based CCC consists of chromates, oxidants, complexants, film agents, etc.. Chromates are the main components in it, and other anions play different roles during the CCC process, e.g. NO^{3-} as oxidant, $C_2O_4^{2-}$ and F^- as film agents. In addition to solution components, immersion time and the anions in the solution all change the characterization of the conversion coating and lead to different anti-corrosion performances[5, 13-17]. Specifically, oxidants in the medium, including perchlorate, permanganate and bichromate, are the key factors affecting the passivation reaction on the alloy surface[18, 19]. But the occurrence of passivation is not simply depending on the oxidability of these reagents. For example, the redox potential of permanganate is more positive than bichromate, but its anti-corrosion efficiency is worse than bichromate on aluminum alloys. Such inconsistence is attributed to the influence of anions. But how these anions affect the passivation properties is still rarely studied.

Li[5] added ZrF_6^{2-}, SO_3^{2-} and BF_4^- into the investigated Cr(III)-based CCC solution, Chen[16] added the F^- in their passivation solution, and Chang[17] induced the hydroxyl alkyl dicarboxylic acid into solution. Fachikov[20] studied the influence of different factors such as concentration, temperature, pH and cathodic polarization on formation, properties and composition of coatings obtained under treatment of zinc surfaces by molybdate solutions. But how these anions affect the passivation properties is still rarely studied.

In this work, we examined the effect of three different anions, i.e. F^-, $C_2O_4^{2-}$ and $Mo_7O_{24}^{6-}$, on the morphology and electrochemical properties of Cr(III)-based CCC on aluminum alloy. The three anions are widespread agents to promote film formation in the conversion coating industry, but their corresponding roles in the conversion coating process are still unclear. Thus, we conducted scanning Electron Microscopy (SEM) observation to study the morphology and structure of the coatings at first. And then, the electrochemical tests, including polarization curve, electrochemical impedance spectroscopy (EIS), were employed to characterize the passivation properties of conversion coating in different solution. Based on the results, we attempt to clarify the underlying mechanisms about the effect of anions, i.e. F^-, $C_2O_4^{2-}$ and $Mo_7O_{24}^{6-}$ on the conversion coating on the aluminum alloy.

2. EXPERIMENTAL

2.1 Materials and samples preparation

The material used in this study was commercial aluminum alloy ADC12 provided from Xinren Technology Company. The specimen surface was successively abraded with 400, 800, 1200, 2000 grit silicon carbide papers at first. Then, it was degreased with acetone for 2 min, ultrasonically cleaned in

ethanol for 2 min, and rinsed in distilled water before activated for 10s in nitric acid solution (pH=2). After activation, it was rinsed in distilled water again and dried in air.

The composition of the passivation bath were 0.01M $Cr(NO_3)_3$, the ratio of Cr(III) salt to the other anions, F^-, $C_2O_4^{2-}$ and $Mo_7O_{24}^{6-}$, was 2/1, and they are noted as Cr(III)/F^-, Cr(III)/$C_2O_4^{2-}$, Cr(III)/MoO_7^{2-} solution, respectively. The solution pH was adjust to the optimal condition by adding corresponding amount of 5M H_2SO_4 into the conversion solution. The Cr(III)-based CCC on aluminum alloy were fabricated by immersing the specimens in the bath for 10 min at room temperature. After immersion, they were rinsed in distilled water for 1 min and dried in the air finally. The solutions are all open to air.

2.2 Electrochemical experiment

The electrochemical experiments were performed in a classical three-electrode cell with 3% NaCl as test solution at room temperature. Aluminum alloy ADC12 was used as working electrode, while a platinum foil and a saturated calomel electrode (SCE) with the Luggin capillary as counter electrode and reference electrode, respectively. The electrochemical measurements were performed the aluminum electrodes with 1 cm^2 exposed surface area at 298 K. EIS measurement was carried out over the frequency range of 100 kHz–10 mHz at the steady open circuit potential (OCP) with an excitation amplitude of 5 mV. The potentiodynamic polarization curves were obtained from -250 mV to +250 mV (versus OCP) with a scan rate of 2 mV/s, the data were collected and analyzed by electrochemical software Zsimpwin. Each experiment was repeated at least three times to check the reproducibility.

2.3 Morphological characterization

The surface morphologies of specimens were observed on a Tescan Vega3 SEM instrument at high vacuum . The accelerating voltage was 20 kV. The contact angles (CA) were measured by sessile water drop method by a contact angle goniometer (Dataphysics OCA20, Germany). The average CA value was obtained by more than five valid measurements on different spots of the same sample.

3. RESULTS AND DISCUSSION

3.1 Superficial morphology

Fig.1 shows the SEM surface morphology of the conversion coating in Cr(III)/F^-, Cr(III)/$C_2O_4^{2-}$, Cr(III)/$Mo_7O_{24}^{6-}$ solution, respectively. These coatings were prepared in corresponding baths with 0.01 M Cr(III) at 25°C for 10min. The specimen in Cr(III)/F^- solution, as shown in Fig.1a, shows slightly smoother morphology. But there are huge amounts of irregular crevices on the surface coats, which are due to water evaporation during the coating formation process[21, 22]. These crevices will become defects on the coat and suffer attack from aggressive ions in the corrosion medium, thus decrease the performance of coating. The coating in Cr(III)/$C_2O_4^{2-}$ (Fig 1b) exhibits similar

morphology as the one in Cr(III)/F^- solution, but the crevices are a bit narrower and shorter. Nevertheless, the specimen in Cr(III)/$Mo_7O_{24}^{6-}$ solution (Fig.1c) displays a much smooth morphology without notable crevices and pores on the coat.

From the SEM micrographs above, we can observed that, the morphology of Cr(III)-based CCC on aluminum alloy is varied among the specimens immersed in different solutions, suggesting the anions significantly affect the property of conversion coating. Thus, we can enhance the specific property of the coating, i.e. corrosion resistance, by adding certain anions into the conversion solution.

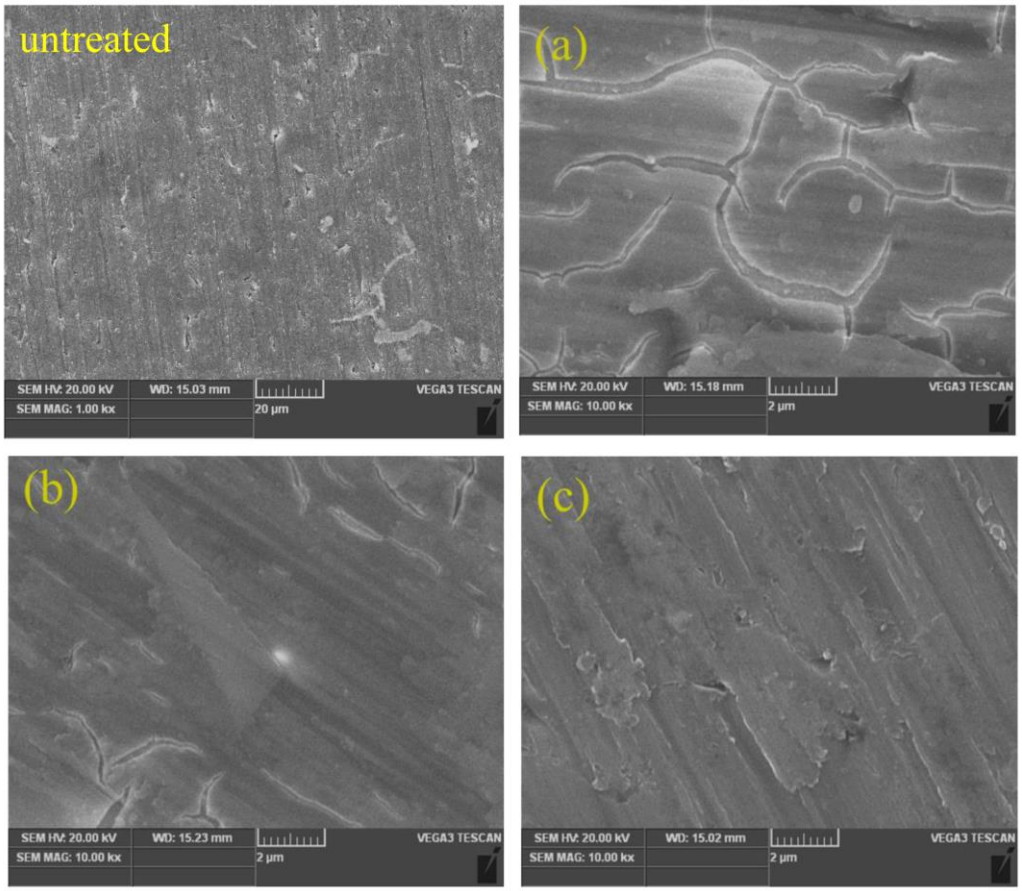

Figure 1. SEM micrographs of the Cr(III)-based CCC in different solutions: (a) Cr(III)/F^-, (b) Cr(III)/$C_2O_4^{2-}$, (c) Cr(III)/MoO_7^{2-} and untreated surface, respectively.

3.2 Potentiodynamic polarization test

Table 1. Potentiodynamic polarization parameters of different Cr(III)-based coating in 3% NaCl solution at 298K

Bath	E_{corr} (V vs. SCE)	β_c (mV dec^{-1})	β_a (mV dec^{-1})	I_{corr} (µA cm^{-2})
blank	-0.654	492.4	33.14	7.85
Cr(III)/F^-	-0.654	302.7	34.52	1.59
Cr(III)/ $C_2O_4^{2-}$	-0.684	168.1	45.24	0.538
Cr(III)/$Mo_7O_{24}^{6-}$	-0.852	36.44	93.06	0.498

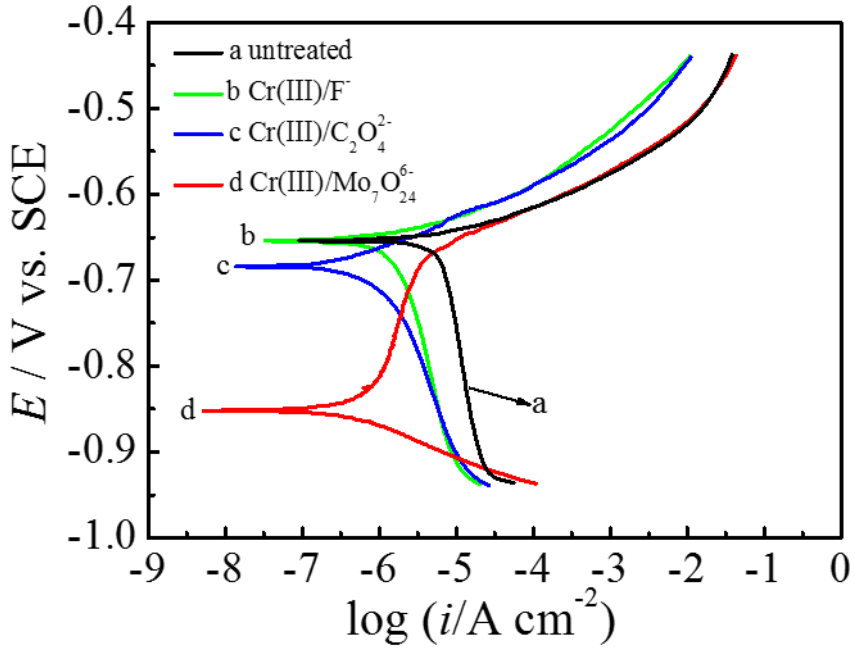

Figure 2. Potentiodynamic polarization curves of the aluminum alloy specimens in 3% NaCl solution. The specimens are treated in different conversion solution, i.e. untreated, (a) Cr(III)/F^-, (b) Cr(III)/ $C_2O_4^{2-}$, and (c) Cr(Ⅲ)/$Mo_7O_{24}^{6-}$.

In order to evaluate the corrosion resistance of the Cr(III)-based coatings on aluminum substrate formed in different conversion solutions, we measured their potentiodynamic polarization curves in 3% NaCl solution at 298 K after the coatings were prepared in corresponding conversion solutions, as shown in Fig. 2. The polarization curve for untreated aluminum specimens is also included as a comparison (black curve in Fig. 2). The corrosion current density (I_{corr}), corrosion potential (E_{corr}) are determined by Tafel extrapolation method[23]. The relevant parameters are listed in Table 1. Based on the results in Fig. 1 the anti-corrosion performance of the coatings rank according to bare substrate < Cr(III)/F^--treated < Cr(III)/ $C_2O_4^{2-}$-treated coating < Cr(Ⅲ)/$Mo_7O_{24}^{6-}$-treated coating.

Corrosion current density (I_{corr}) is often used to evaluate the corrosion protective property of the coatings. As shown in Table 1, compared with the bare substrate, the aluminum immersed in Cr(III)/F^- solution has a lower corrosion current density (I_{corr}). At the same time, I_{corr} for the Cr(III)/$C_2O_4^{2-}$-treated coating is decreased approximately by one order of magnitude contrast to the bare substrate. Furthermore, I_{corr} for the Cr(Ⅲ)/$Mo_7O_{24}^{6-}$-treated coating is decreased more than others. Besides, an onset passive region amounted to 120 mV was observed for the Cr(Ⅲ)/$Mo_7O_{24}^{6-}$ solution. The presence of long perfect passive region suggests that the Cr(Ⅲ)/$Mo_7O_{24}^{6-}$-treated coating is considerably uniform, pore-free and adherent as well as high protective in Cl^- containing solution.

As we can observed in Fig.2, the specimens treated in Cr(Ⅲ)/$Mo_7O_{24}^{6-}$ solution displays the most negative corrosion potential (-0.852V vs SCE), which decrease 198mV compared to the one which without treated. According to A. Conde et al.[24] , the increased coverage of insoluble salts leads the corrosion potential decreased. Thus, the decrease of corrosion potential demonstrates the formation of increased insoluble salt ($Cr(OH)_3$/Cr_2O_3) on the aluminum alloy (We discussed in section

3.5). As observed in Table 1, we can see the corrosion potential all decreased, and the decreasing tendency is Cr(III)/F^--treated < Cr(III)/ $C_2O_4^{2-}$-treated coating < Cr(Ⅲ)/$Mo_7O_{24}^{6-}$-treated coating. It indicates the increased composition of $Cr(OH)_3$/Cr_2O_3 in coating. Furthermore, it implies the $Mo_7O_{24}^{6-}$ is best during the three film agents.

3.3 Electrochemical impedance spectroscopy (EIS)

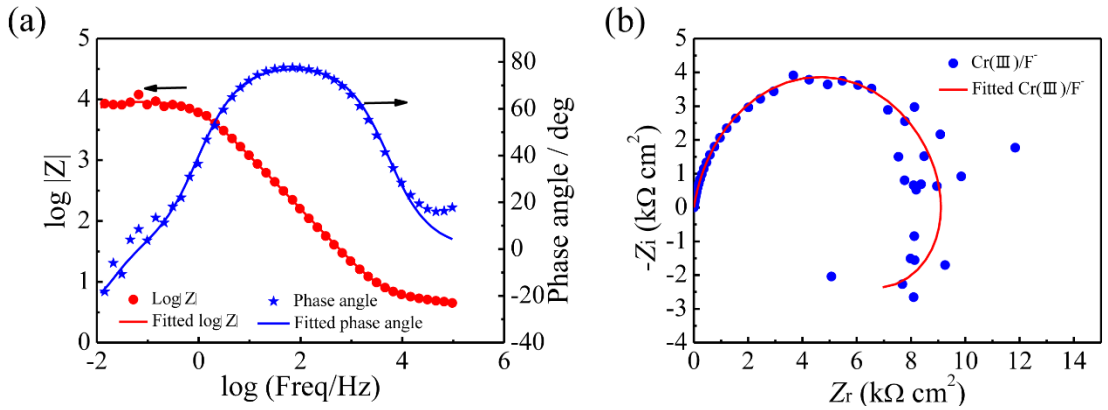

Figure 3. Impedance responses for aluminum alloy in 3% NaCl solution with at 298K after being treated with Cr(III)/F^- solution. (a) Bode plot; (b) Nyquist plot.

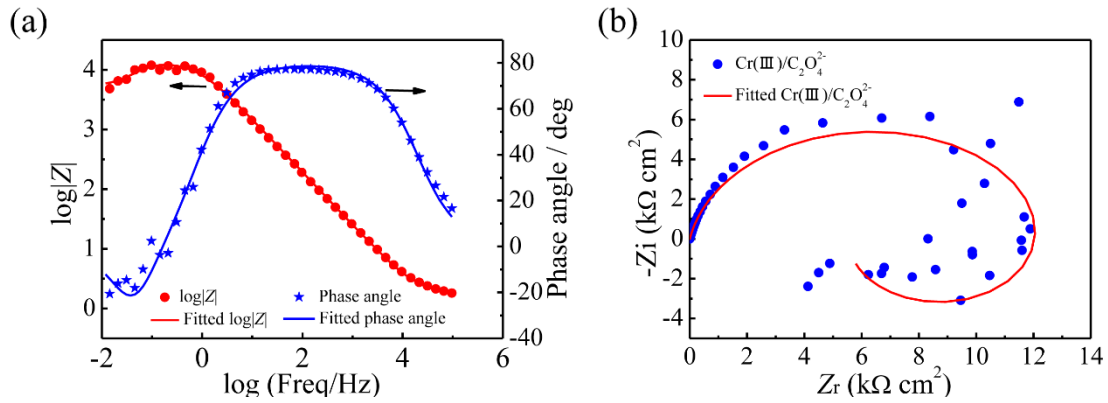

Figure 4. Impedance responses for aluminum alloy in 3% NaCl solution at 298K after being treated with Cr(III)/$C_2O_4^{2-}$ solution. (a) Bode plot; (b) Nyquist plot.

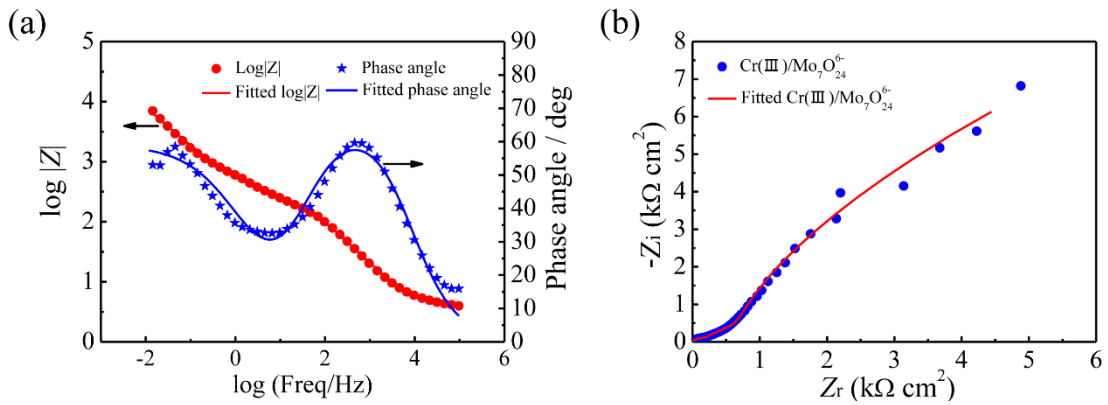

Figure 5. Impedance responses for aluminum alloy in 3% NaCl solution at 298K after being treated with Cr(Ⅲ)/$Mo_7O_{24}^{6-}$ solution, (a) Bode plot; (b) Nyquist plot.

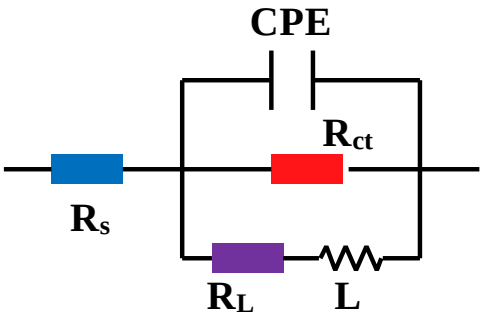

Figure 6. The equivalent circuit model used to fit the EIS experiment data for Cr(III)/F^- and Cr(III)/$C_2O_4^{2-}$ solutions.

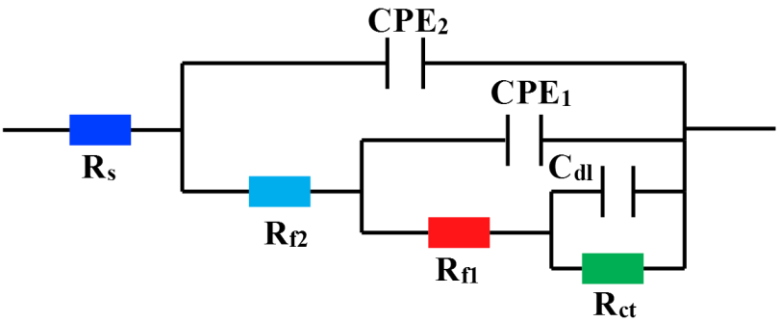

Figure 7. The equivalent circuit model used to fit the EIS experiment data for Cr(III)/$Mo_7O_{24}^{6-}$ solution

Table 2. EIS parameters of aluminum alloy in 3% NaCl solution at 298K after being treated in different passivation solution

Bath	R_s (Ω cm^2)	CPE		R_L (Ω cm^2)	L (H cm^2)	R_{ct} (kΩ cm^2)
		Y (μF/cm^2)	n			
Cr(III)/F^-	4.78	21.4	0.879	8304	2.409E5	9.32
Cr(III)/ $C_2O_4^{2-}$	1.78	16.8	0.887	9687	5.517E4	12.9
Cr(III)/$Mo_7O_{24}^{6-}$	3.78	8.80	1.00	-	-	38.8

We also conducted the EIS measurement for the aluminum alloy in 3% NaCl solution after treatment in different conversion solution to further explore the effect of these adding anions. Fig. 3 shows Bode (Fig. 3a) plot and Nyquist plot (Fig. 3b) of the aluminum alloy in 3% NaCl medium at 298K after being treated with Cr(III)/F^- solution. Its phase plot (blue hollow star in Fig. 3a) indicates there has a time constant over the measured frequency as indicated with black arrow, which is characterized with interface capacitance and also has a inductance effect at low frequency region. Additionally, its absolute impedance plot (red hollow circle in Fig.3) displays a maximum value of $10^{3.9}$ Ω cm^2 for the faraday admittance (Z_w). The conclusion above can be verified from the Nyquist plot, which includes one capacitance arc and one inductance arc at high frequency region and low frequency region, respectively. .

It is also necessary to model the impedance data with an equivalent circuit to extract more information about the structure and corrosion resistance of the coatings. According to the above analysis, the equivalent circuit in Fig.6 was used to fit the impedance response of aluminum alloy treated with Cr(III)/F^- solution. In this circuit, R_s denotes the electrolyte resistance, CPE is constant phase angle element, and L is the inductance element. R_{ct} and R_L represent the charge transfer resistance and the inductance resistance, respectively. It is obvious that the fitting values (curves in Fig.3a-b) coincided greatly with the experimental results (star and circle in Fig.3a-b), indicating this equivalent circuit is appropriate for the impedance response of aluminum alloy treated in Cr(III)/F^- solution. There are quite some factors to cause the appearance of the inductance at low frequency[25]. But in this system, we believe it is due to the formation of pores on the metal surface as observed with SEM examination. The defects on the coating exist as defects and become active site for corrosion reaction in aggressive solution. Such variation leads to the appearance of inductive arc.

The Bode (Fig. 4a) and the Nyquist plots (Fig. 4b) for the Cr(III)-based CCC on aluminum alloy after being treated with Cr(III)/$C_2O_4^{2-}$ solution are shown in Fig.4. We can observed that its impedance responses are similar to that treated with Cr(III)/F^- solution (Fig.3). So the equivalent circuit in Fig.6 is also suitable for the impedance responses of specimens treated in Cr(III)/$C_2O_4^{2-}$ system. But the maximum value of faraday admittance (Z_w) increased. As for inductive arc in this case, in addition to the presence of defects in the coating, the intermediate product, due to the existence of $C_2O_4^{2-}$, as shown in reaction 8, might be another factor to cause the system variation at low frequency. Fig.5 shows the Bode (Fig. 5a) and the Nyquist plot (Fig. 5b) of the aluminum alloy in 3% NaCl solution after treatment in Cr(III)/$Mo_7O_{24}^{6-}$ solution, which is total different from the impedance responses in another two system above. Its phase plot (blue hollow star in Fig. 5a) is characterized with two time constants and the maximum value in absolute impedance plot (red hollow circle in Fig. 5a) is more than others. The equivalent circuit of Cr(III)/$Mo_7O_{24}^{6-}$-treated system is shown in Fig. 7, R_s stands for the electrolyte resistance, R_n and CPE_n (n=1–2) are resistive responses and constant phase angle elements, respectively, of the nth layer of Cr(III) conversion coatings. R_{ct} and C_{dl} represent, the charge transfer resistance and electrical double layer capacitance, respectively.

The constant phase element (CPE) and the diffusion elements can respond the potential fluctuation in the coating formation process. And they are the main components used to construct the equivalent circuit of the conversion coatings. A conversion coating may includes several heterogeneous layers. One heterogeneous layer can be expressed as a parallel circuit containing two branches in an equivalent circuit: a nonideal capacitance (Q), and a resistance (R). The nonideal capacitance is called the constant phase element. Therefore, the equivalent circuit of a conversion film including n heterogeneous layers would contain n parallel CPEs[12]. This principle has been wildly applied to create the equivalent circuit of the conversion coatings by many researchers[26-28]. So we can see from Figure 7 that Cr(III)/$Mo_7O_{24}^{6-}$-treated conversion coating had a dense and two layers structure, it also reveals that Cr(III)/$Mo_7O_{24}^{6-}$-treated conversion coating is more effective than others, and $Mo_7O_{24}^{6-}$ is the best coating formation agent among the three anions.

Table 2 listed the extracted parameters from the equivalent circuit for each impedance plot. The value of R_{ct} represents the charge transfer between the solution and the electrode. We can observe that R_{ct} increase from 9321 Ω cm^2 and 12960 Ω cm^2 to 38860 Ω cm^2 as the adding anions change from F^-

and $C_2O_4^{2-}$ to $Mo_7O_{24}^{6-}$. While the Y_0 value exhibits reverse dependence, from 2.14×10^{-5} to 8.80×10^{-6}, which is due to the coverage on the aluminum surface by the promotion of film agents. The decreased values of Y_0 indicates the reducing in local dielectric constant or an increase in the thickness of the dielectric double layer, suggesting that $Mo_7O_{24}^{6-}$ is the best agent to promote the formation of conversion coating.

Based on the discussion above, we can conclude that when $Mo_7O_{24}^{6-}$ are added into the Cr(III)-based conversion solution, the coating on aluminum alloy could keep intact and also exhibit maximum corrosion resistance. Thus, $Mo_7O_{24}^{6-}$ is better coating formation agent than F^- and $C_2O_4^{2-}$.

3.4 Contact angle measurement

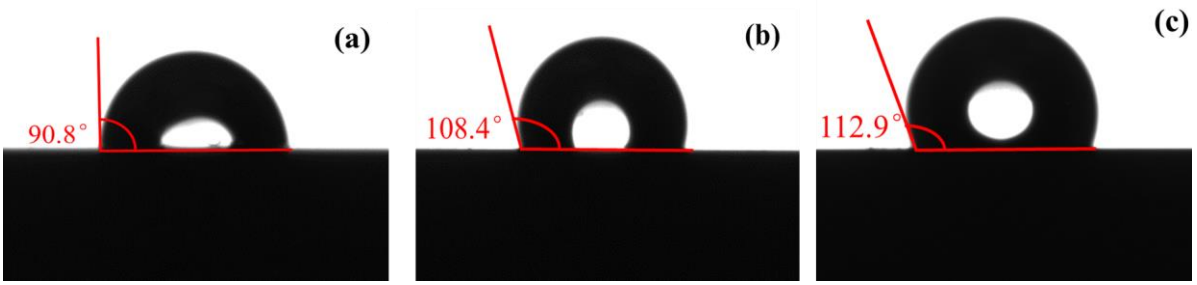

Figure 8. Sessile water drop images on aluminum surface after treated with different solutions: (a) Cr(III)/F^-, (b) Cr(III)/ $C_2O_4^{2-}$, (c) Cr(III)/$Mo_7O_{24}^{6-}$.

Generally, the value of contact angle strongly and mainly depends on the properties of surface. Therefore, the contact angle measurement was used to further explore the effect of three different anions. The wettability of aluminum surface after treated with Cr(III)/F^- solution, Cr(III)/$C_2O_4^{2-}$ solution and Cr(III)/$Mo_7O_{24}^{6-}$ solution were examined by measuring the contact angle is shown in Figure 8. We can see that aluminum alloy treated with Cr(III)/F- solution has a hydrophilic surface for the contact angle is 90.8° (Fig. 8a), while the angle on the Cr(III)/$C_2O_4^{2-}$ coated surface is 108.4° (Fig. 7b) and Cr(III)/$Mo_7O_{24}^{6-}$ coated surface is 112.9° (Fig. 8c). It is clear that the contact angles gradually increase as the adding anions change from F^- and $C_2O_4^{2-}$ to $Mo_7O_{24}^{6-}$. Moreover, the maximum value of contact angle is present when added the $Mo_7O_{24}^{6-}$ into solution. Thus, the anions affect the properties of conversion coating significantly.

3.5 Formation mechanism

For the aluminum alloy treated in Cr(III) solution, the production and transformation formula of the conversion coatings are shown as follows:

Cathode reaction: $O_2 + 2H_2O + 4e^- \rightarrow 4OH^-$ (R1)

Anode reaction: $Al \rightarrow Al^{3+} + 3e^-$ (R2)

The cathodic hydrogen evolution (reaction 1) leads to the increase of pH value on the aluminum surface. Thus, for the aluminum alloy treated in Cr(III) solution, chromium oxide/hydroxide

($Cr(OH)_3/Cr_2O_3$) and aluminum oxide/hydroxide ($Al(OH)_3/Al_2O_3$), as shown below, are formed near the surface and deposit thereon.

$$Al^{3+} + 3OH^- \rightarrow Al(OH)_3 \quad \text{(R3)}$$

$$Cr^{3+} + 3OH^- \rightarrow Cr(OH)_3 \quad \text{(R5)}$$

$$Cr^{3+} + 6OH^- \rightarrow Cr_2O_3 \quad \text{(R6)}$$

The formation of $Cr(OH)_3/Cr_2O_3$ and $Al(OH)_3/Al_2O_3$ retard the reaction of cathodic reaction, leading to the decrease of current density. If F^- is added into the conversion solution, the cathodic reaction will be complemented as reaction 7:

$$Al^{3+} + 3F^- \rightarrow AlF_3 \quad \text{(R7)}$$

In the aqueous solution, the Cr^{3+} ions exist as $[Cr(H_2O)_6]^{3+}$, an inner orbital coordination compound whose outer valent d-orbit by occupied the lone-pair electrons of H_2O. Thus, the $[Cr(H_2O)_6]^{3+}$ is hardly to react with the reagent in the conversion solution for coating formation during the passivation process[29-32]. However, in the presence of $C_2O_4^{2-}$, the ligand ions of $C_2O_4^{2-}$ expand the distance between Cr^{3+} ion and the H_2O molecules (r) and exposed the ions of Cr^{3+}, as reaction 8:

$$\left[Cr(H_2O)_6(C_2O_4^{2-})\right]^+ \rightarrow Cr^{3+} + C_2O_4^{2-} + 6H_2O \quad \text{(R8)}$$

The unconstrained ions of Cr^{3+} could inhibit the anodic dissolution of chromium , and also react with OH^- to deposit on the specimen surface as $Cr(OH)_3/Cr_2O_3$ for coating formation, which suppress the cathodic hydrogen evolution. Thus, both cathodic and anodic current density of Cr(III)-based coating formed in $Cr(III)/C_2O_4^{2-}$ solution reduced.

Additionally, if added the $Mo_7O_{24}^{6-}$ into the solution, it can not only react with H^+ to generate MoO_3 on the specimen surface[33], but also accumulate OH^- to promote the precipitation of $Cr(OH)_3/Cr_2O_3$.

$$Mo_7O_{24}^{6-} + 6H^+ \rightarrow 7MoO_3 + 3H_2O \quad \text{(R9)}$$

We can conclude that the addition of film agents into the conversion solution improved the corrosion resistance of Cr(III)-based coating on the aluminum alloy. But the coatings performance are various due to the different effects of three anions. And all results demonstrate $Mo_7O_{24}^{6-}$ is the best coating formation agent among the three anions.

4 CONCLUSIONS

We studied the effect of three different anions, i.e. F^-, $C_2O_4^{2-}$ and $Mo_7O_{24}^{6-}$, on the morphology and the electrochemical properties of Cr(III)-based CCC on aluminum alloy. The SEM micrographs and contact angle measurements observed that the morphology and property of Cr(III)-based CCC on aluminum alloy are varied due to the addition of different anions into conversion solutions, and the specimen in $Cr(III)/Mo_7O_{24}^{6-}$ solution exhibits a much smooth and dense morphology than the ones in $Cr(III)/F^-$ and $Cr(III)/C_2O_4^{2-}$ solutions. The electrochemical measurements showed that F^-, $C_2O_4^{2-}$ and

$Mo_7O_{24}^{6-}$ have different functions during the CCC process. We believed that F^- can formed one more component for coating formation, that the presence of $C_2O_4^{2-}$ could release the ions of Cr^{3+} and accelerated the deposition of insoluble salts, and that the $Mo_7O_{24}^{6-}$ can not only react with H^+ but also promote the precipitation of $Cr(OH)_3/Cr_2O_3$. Above all, $Mo_7O_{24}^{6-}$ is the best coating formation agent among the three anions.

ACKNOWLEDGEMENTS
This work was supported by Natural Science Foundation of China (No. 21376282)

Reference

1. Y. Totik, R. Sadeler, I. Kaymaz, M. Gavgali. *J Mater Process Tech*, 147 (2004) 60.
2. B. E. Rivera, B. Y. Johnson, M. J. O'Keefe, W. G. Fahrenholtz. *Surf Coat Tech*, 176 (2004) 349.
3. C. Y. Bai, Y. H. Chou, C. L. Chao, S. J. Lee, M. D. Ger. *Journal of Power Sources*, 183 (2008) 174.
4. O. Lunder, J. C. Walmsley, P. Mack, K. Nisancioglu. *Corros Sci*, 47 (2005) 1604.
5. L. L. Li, G. M. Swain. *Acs Appl Mater Inter*, 5 (2013) 7923.
6. L. Q. Zhu, F. Yang, N. Ding. *Surf Coat Tech*, 201 (2007) 7829.
7. R. Berger, U. Bexell, T. M. Grehk, S. E. Hornstrom. *Surf Coat Tech*, 202 (2007) 391.
8. A. C. Bastos, M. G. Ferreira, A. M. Simoes. *Corros Sci*, 48 (2006) 1500.
9. T. Y. Chen, W. F. Li, J. Cai. *Rsc Adv*, 1 (2011) 607.
10. W. R. McGovern, P. Schmutz, R. G. Buchheit, R. L. McCreery. *J Electrochem Soc*, 147 (2000) 4494.
11. E. Akiyama, A. J. Markworth, J. K. McCoy, G. S. Frankel, L. Xia, R. L. McCreery. *J Electrochem Soc*, 150 (2003) B83.
12. N. T. Wen, C. S. Lin, C. Y. Bai, M. D. Ger. *Surf Coat Tech*, 203 (2008) 317.
13. S. Pommiers-Belin, J. Frayret, A. Uhart, J. Ledeuil, J. C. Dupin, A. Castetbon, et al. *Appl Surf Sci*, 298 (2014) 199.
14. S. L. Mu, W. F. Li, J. Du. *Electrochim Acta*, 125 (2014) 580.
15. W. K. Chen, J. L. Lee, C. Y. Bai, K. H. Hou, M. D. Ger. *J Taiwan Inst Chem E*, 43 (2012) 989.
16. W. K. Chen, C. Y. Bai, C. M. Liu, C. S. Lin, M. D. Ger. *Appl Surf Sci*, 256 (2010) 4924.
17. Y. T. Chang, N. T. Wen, W. K. Chen, M. D. Ger, G. T. Pan, T. C. K. Yang. *Corros Sci*, 50 (2008) 3494.
18. F. Yu, W. F. Li, X. P. Chen, G. G. Zhang. *Mater Res Innov*, 19 (2015).
19. S. Y. Jian, Y. R. Chu, C. S. Lin. *Corros Sci*, 93 (2015) 301.
20. L. Fachikov, D. Ivanova. *Appl Surf Sci*, 258 (2012) 10160.
21. L. J. Li, J. L. Lei, S. H. Yu, Y. J. Tian, Q. Q. Jiang, F. S. Pan. *J Rare Earth*, 26 (2008) 383.
22. A. A. Zuleta, E. Correa, C. Villada, M. Sepulveda, J. G. Castano, F. Echeverria. *Surf Coat Tech*, 205 (2011) 5254.
23. X. W. Zheng, S. T. Zhang, W. P. Li, M. Gong, L. L. Yin. *Corros Sci*, 95 (2015) 168.
24. A. Conde, M. A. Arenas, A. de Frutos, J. de Damborenea. *Electrochim Acta*, 53 (2008) 7760.
25. V. Freger. *Electrochem Commun*, 7 (2005) 957.
26. Y. J. Tan, S. Bailey, B. Kinsella. *Corros Sci*, 38 (1996) 1545.
27. H. P. Duan, K. Q. Du, C. W. Yan, F. H. Wang. *Electrochim Acta*, 51 (2006) 2898.
28. T. K. Rout. *Corros Sci*, 49 (2007) 794.

29. N. V. Phuong, S. C. Kwon, J. Y. Lee, J. H. Lee, K. H. Lee. *Surf Coat Tech*, 206 (2012) 4349.
30. N. V. Phuong, S. C. Kwon, J. Y. Lee, J. Shin, B. T. Huy, Y. I. Lee. *Microchem J*, 99 (2011) 7.
31. Z. X. Zeng, Y. L. Sun, J. Y. Zhang. *Electrochem Commun*, 11 (2009) 331.
32. N. V. Mandich, C. C. Li, J. R. Selman. *Plat Surf Finish*, 84 (1997) 82.
33. S. L. Mu, J. Du, H. Jiang, W. F. Li. *Surf Coat Tech*, 254 (2014) 364.